Am J Cancer Res 2020;10(6):1900-1918
www.ajcr.us /ISSN:2156-6976/ajcr0113297

Original Article

BRIT1 dysfunction confers synergistic inhibition of hepatocellular carcinoma by targeting poly (ADP-ribose) polymerases and PI3K

Yulong Liang[1*], Lihou Yu[1*], Dongxiao Zhang[2], Xuemei Zhao[3], Hong Gao[1], Betty L Slagle[4], John A Goss[1], Xiaosong Wang[5], Kaiyi Li[1], Shiaw-Yih Lin[6]

[1]The Michael E. DeBakey Department of Surgery, Baylor College of Medicine, Houston, TX, USA; [2]Beijing Hospital of Traditional Chinese Medicine, Capital Medical University, Beijing, China; [3]School of Pharmaceutical Science, Shandong First Medical University, Tai'an, Shandong, China; [4]Department of Molecular Virology and Microbiology, Baylor College of Medicine, Houston, TX, USA; [5]UPMC Hillman Cancer Center, Department of Pathology, University of Pittsburgh, Pittsburgh, PA, USA; [6]Department of Systems Biology, UT MD Anderson Cancer Center, Houston, TX, USA. [*]Equal contributors.

Received April 25, 2020; Accepted May 1, 2020; Epub June 1, 2020; Published June 15, 2020

Abstract: BRIT1 has emerged as a novel key player in homologous recombination (HR). It is located in 8p23, a locus frequently deleted in hepatocellular carcinoma (HCC). Previously, we found that BRIT1-deficiency triggered genomic instability and tumor formation in our mouse model. Here we aim to determine whether BRIT1 aberrations are implicated in HCC and, if so, whether they can be used for targeted therapy with PARP inhibitors and other agents. We analyzed HCC samples for BRIT1 alterations at DNA, RNA and protein levels. BRIT1 was found deleted and/or downregulated in ~30% of HCC samples; BRIT1 mutant K659fsX10 identified in HCC abolished DNA repair function. Notably, BRIT1 deletion was correlated with poor survival and high recurrence of HCC. To determine the role of BRIT1 deficiency in potentiating the drug response, we subsequently generated BRIT1-deficient HCC cells, determined their HR defects, and assessed their response to the PARPi olaparib and PI3K inhibitor in vitro and in mice. BRIT1-deficient HCC cells were HR defective and hypersensitive to olaparib alone or in combination with PI3K inhibitor BEZ235, both in vitro and in vivo. The cytotoxicity of olaparib alone or in combination with BEZ235 was largely alleviated by ectopic BRIT1. We also found that BEZ235 markedly enhanced the production of poly (ADP-ribose) and the level of double-strand breaks (DSB) and single-strand breaks (SSB) in BRIT1-deficient cells. In summary, our results identify BRIT1 deficiency as a potential driver for HCC development, and BRIT1 status is critical to sensitivity to treatment with olaparib and/or BEZ235. PI3K inhibition induces substantial DNA damage and makes cells more dependent on PARP activity in the context of BRIT1 deficiency, thus, BRIT1 depletion facilitates enhancing synthetic lethality of PARP inhibitors and PI3K inhibitors in HCC. This study provides a new mechanistic foundation for significantly expanding the application of PARPi in HCC therapy.

Keywords: BRIT1/MCPH1, liver cancer, homologous recombination, targeted therapy, combination therapy, PARP inhibitor, PI3K inhibitor

Introduction

BRIT1 (also known as MCPH1) has recently been identified as a novel key player in the DNA damage response (DDR) [1-6]. BRIT1 belongs to a protein family sharing BRCA1 C-terminal (BRCT) domains [7]. It contains three BRCT domains, one in N-terminus (N-BRCTs) and two in C-terminus (C-BRCTs). The C-BRCTs of BRIT1 are necessary for self-oligomerization, ionizing radiation (IR)-induced nuclear foci formation, and recruitment of BRCA2/RAD51 and other DNA repair proteins to the DNA damage sites for execution of DNA repair function [2-4]. Cells with ablation of BRIT1 are more sensitive to IR with increased chromosomal abnormalities. Our recent studies showed that BRIT1 is essential for homologous recombination (HR) DNA repair and acts as a critical tumor barrier via maintenance of genomic integrity using our

BRIT1$^{-/-}$ mouse model [8, 9]. Meanwhile, human chromosome locus 8p23, where the BRIT1 gene is located, has been observed to be frequently deleted in hepatocellular carcinoma (HCC) [10, 11]. Together these observations suggest that BRIT1 deficiency might be implicated in the formation of HCC, which however, remains ill understood.

HCC is the 3rd leading cause of cancer mortality worldwide and advanced HCC has a poor 5-year survival rate of below 15% [12, 13]. Effective therapeutic options for advanced HCC, including targeted therapy for advanced cases, are highly limited [14, 15]. Tyrosine kinase inhibitors sorafenib and regorafenib are the only two main targeting drugs approved by the Food and Drug Administration for treating advanced HCC, yet the benefit of this treatment is very marginal [16]. Recently, poly (ADP-ribose) polymerase (PARP) inhibitor (PARPi)-based synthetic lethality has emerged as a targeted therapy for HR-deficient cancers caused by BRCA1/2-mutations [17]. PARPs are a family of enzymes that are activated by single- and double-strand breaks (SSBs and DSBs) and share the ability to poly(ADP-ribosyl)ate protein substrates [18]. Inhibition of PARPs by PARPi induces accumulation of many unrepaired SSBs which leads to the collapse of replication forks during the S phase and subsequently to DSBs. These DSBs during S phase would be normally repaired by HR, but in cells with defective HR, such as BRCA1/2-mutated cells, DSBs tend to be repaired by an error-prone, non-homologous end joining (NHEJ), leading to deleterious DNA damages, which in turn cause cell death [17]. In addition to accumulation of unrepaired SSBs caused by PARP inactivation, PARPi traps the PARP1 and PARP2 enzymes at damaged DNA [19] and the trapped PARP-DNA complexes cause additional severe cytotoxicity in cells [20]. Thus, PARPi instigate synthetic lethality in HR-deficient cells and presently, this class of compounds are being used for treating HR-deficient breast and ovarian cancer patients in clinic [21]. In HCC, the key players in HR such as BRCA1/2 exhibit a very low rate of mutation and aberrant expression, which limits the application of PARPi in HCC. However, the locus of BRIT1, a novel key player of HR, is frequently deleted in HCC [10, 11].

In this study, we sought to determine whether BRIT1-deficient HCC is HR defective and, if so, whether HCC carrying BRIT1-deficiency can be targeted by PARPi as a single agent or in combination with other anticancer drugs. We investigated whether BRIT1 alterations are implicated in HCC and whether its aberrations can represent a novel therapeutic target. We observed that BRIT1 is deleted and/or low-expressed in a significant number of HCC samples. BRIT1 deletion was positively correlated with poor prognosis of HCC. Moreover, BRIT1-deficient cells were hypersensitive to PARPi alone or in combination with PI3Ki in vitro and in vivo, and the synergistic action could be largely reversed by ectopically expressed BRIT1. Our findings provide proof-of-concept evidence that BRIT1 deficiency can be targeted by PARPi, potentially expanding its usage in treatment of HCC irrespective of BRCA status.

Materials and methods

Human samples, animals, cell lines, and reagents

Human hepatocellular carcinoma (HCC) samples and matched adjacent noncancerous liver tissues (35 sets) were obtained from Qidong Liver Cancer Institute (Qidong, Jiangsu, China) and the Liver Center at Baylor College of Medicine (BCM, Houston, TX, USA) through collaboration with Drs. Betty L. Slagle and John A. Goss, respectively. Informed consent for the studies to be performed was obtained in accordance with the guidelines of the local ethics committee. The features of this sample population have been previously described [22-24]. All animals used in this study received humane care according to the criteria outlined in the *Guide for the Care and Use of Laboratory Animals*. Nude mice were obtained from the Jackson Laboratory (Bar Harbor, ME). Animal protocol (AN-3142) was approved by the Institutional Animal Care and Use Committee (IACUC) at BCM. We used mice 6-8 weeks of age for in vivo studies. HCC cell lines Huh7, Hep3B, and HepG2 were purchased from the American Type Tissue Collection (Manassas, VA), and cultured in DMEM with standard supplements (Life Technologies, Grand Island, NY). HCC cell lines SNU-182, SNU-423, and SNU-449 were kindly provided by Dr. Thomas D. Schmittgen (Ohio State University, Columbus, OH), and cultured in RPMI 1640 with standard supplements (Life Technologies, Grand Island, NY). BRIT1$^{+/+}$ and BRIT1$^{-/-}$ mouse embryonic

fibroblasts (MEFs) were generated as described previously [8]. All cells were maintained at 37°C with 5% CO_2. PARP inhibitors olaparib and AG014699, and the PI3K inhibitor NVP-BEZ235 were purchased from Selleck Chemicals (Houston, TX).

Isolation of genomic DNA, RNA and proteins

Genomic DNA of normal and cancerous tissues or cultured cells was extracted following the standard phenol-chloroform protocol. Total RNA was isolated and prepared with the QIAGEN RNAeasy Plus Mini Kit according to the manufacturer's protocol; and proteins in tissues and cultured cells were lysed in RIPA buffer.

Loss of heterozygosity (LOH) assay

LOH assay was performed with minor modifications as described previously [25]. A total of 13 sequence-tagged site (STS) markers in the BRIT1 locus were selected according to the UCSC Genome Browser on Human Feb. 2009 (GRCh37/hg19) Assembly (www.genome.ucsc.edu), and are listed below: SHGC-18315 (STS1, or S1), RH92650 (S2), RH48380 (S3), WI-13831 (S4), A004X20 (S5), RH47768 (S6), G59875 (S7), WIAF2168 (S8), RH69270 (S9), D8S277 (S10), SHGC-148851 (S11), SHGC-77726 (S12), SHGC-13858 (S13). The primer sequences specific for these markers are available from GeneCards (http://genecards.weizmann.ac.il/geneloc/index.shtml). Each marker was amplified by PCR. After completion of PCR, the products were run on a 6% polyacrylamide gel electrophoresis (PAGE) gel and then stained with the SilverXpress® Silver Staining Kit (Life Technologies, Grand Island, NY). The band patterns of tumor and noncancerous tissue were compared. Tumor samples with loss of at least one STS marker in the locus of BRIT1 was regarded as LOH positive.

Data mining

HCC datasets (TCGA Provisional or others) were used for data mining with Oncomine [25] or cBioPortal for Cancer Genomics [26]. In this study, we focused on the analysis of the implication of BRIT1 aberrations in HCC. All searches were performed according to the online instructions of the Oncomine and cBioPortal unless otherwise indicated.

Mutation analysis

Complete coding sequences and exon/intron boundaries of the BRIT1 gene were amplified using the Pfx polymerase system (Life Technologies, Grand Island, NY). PCR products were directly sequenced (SeqWright, Houston, TX) or cloned into the Zero Blunt® TOPO® PCR Cloning Kit (Life Technologies, Grand Island, NY) for sequencing. The whole sequence of the identified mutant p.K659MdelfsX10 (or c.1974_1980del) and the sequence spanning the affected splicing acceptor site have been deposited in GenBank (Accession # KU674825 and KU550240). PCR primers used here will be provided upon request.

Nuclear foci formation assay

Cells in culture were treated with olaparib (2.5 μM) or BEZ235 (2.5 nM) for the indicated times, and then collected to perform the nuclear foci formation assay, as described elsewhere [1]. The primary antibodies used here were anti-BRIT1 (8) and anti-γ-H2AX (Bethyl Laboratories, Montgomery, TX; Catalog number A300-081). The coverslips were mounted onto glass slides with VectaShield antifade (Vector Laboratories, Burlingame, CA) and visualized with a Zeiss Axiovert 40 CFL fluorescence microscope (Zeiss, Oberkochen, Germany). These experiments were performed in triplicate for data analysis.

Cell viability and combination index (CI) analysis

Cell viability was determined with the Cell Counting Kit-8 (CCK-8) proliferation assay (Sigma-Aldrich, St. Louis, MO), according to the manufacturer's instruction, and/or with the colony formation assay. Cells (0.5-1 × 10^3) were seeded into 96-well plates and cultured for 5 days for the CCK-8 assay, or seeded into and cultured for 2-4 weeks in 6-well plates for the cologenic assay. Olaparib (0, 1.25, 2.5, 5, 10 μM) or BEZ235 (0, 1.25 2.5, 5, 10 nM) were used in this study. The concentration of drugs required to obtain 50% inhibition (IC50) of proliferation of Hep3B was used to test the effect of the combination therapy of olaparib and BEZ235 in the indicated cells. For 2.5 μM olaparib (~IC50 for Hep3B), 1.25 nM and 2.5 nM BEZ235 were added and for 2.5 nM BEZ235 (~IC50 for Hep3B), 1.25 μM and 2.5 μM olapa-

rib were added. All experimental points were quantified sixfold. Every single point was compared with its respective control value with the same amount of DMSO. All experiments were repeated three times. The inhibitory effect obtained with the combination treatment of olaparib and BEZ235 was analyzed with CI according to the method developed by Chou and Talalay [27-29]. CI values below 0.9 indicate a synergistic effect, 0.9 to 1.1 an additive effect, and above 1.1 an antagonistic effect [29].

Neutral-pH Comet assay

The neutral-pH Comet assay was performed as described previously [9]. Cells were treated with BEZ235 at the different doses for 24 h and then subjected to the neutral-pH Comet assay. Tail moments were determined in at least 75 cells/slide with the Comet Assay IV software (Perceptive Instruments, Bury St Edmunds, UK). Data were collected from three independent experiments.

Apoptosis analysis with flow cytometry

Fluorescence-activated cell sorter (FACS) analysis was used to determine cell apoptosis. Briefly, adherent cells were collected by trypsinization and combined with cells floating in the medium, fixed by 75% ethanol, and then kept at -20°C for at least 2 h. Cells were next stained with propiduim iodide (2 μg/ml in phosphate-buffered saline) and RNase A (10 μg/ml). Flow cytometry was performed with a FACScan (BD Biosciences, San Jose, CA) and data were analyzed with Flowjo software (Tree Star, Ashland, OR). The apoptotic cells were represented by the fraction of the cells with sub-G1 DNA content.

Western blot analysis

Total cell extracts were separated with SDS-PAGE, transferred to nitrocellulose membrane and probed with antibodies against human BRIT1 [8], PAR (IBL-America, Minneapolis, MN; catalog number: 10407), PARP1 (BD Biosciences, San Jose, CA; catalog number: 51-6639GR), phospho-AKT (T308) (Cell Signaling Technology, Danvers, MA; catalog number: 9275), β-actin (Sigma-Aldrich, St. Louis, MO; catalog number: A5044), and α-Tubulin (Sigma-Aldrich, St. Louis, MO; catalog number: T5168). Data are analyzed from three independent experiments.

Xenograft tumor model in vivo

Hep3B, Hep3B.BRIT1, HepG2, and HepG2.BRIT1 cells (1×10^6) pre-mixed with Matrigel Matrix (BD Biosciences, San Jose, CA) were subcutaneously injected into nude mice. After the tumors reach around 100 mm^3 within 2-4 weeks, mice were randomly divided into 4 groups: control (Ctrl), olaparib (OLA), BEZ235 (BEZ), and olaparib in combination with BEZ235 (OLA+BEZ). Olaparib (100 mg/kg, i.p.) and BEZ235 (40 mg/kg, oral administration) were administered alone or in combination every day for 3 weeks. Tumor sizes were measured twice a week with an electrical caliper, and the tumor volume calculated with the following equation: $V=\pi/6 * (length * width^2)$ (V is the tumor volume). Mice were sacrificed when tumors reached 1.5 cm in length, and tumor samples were weighted and fixed or snap-frozen in liquid nitrogen and stored at -80°C for future use.

Immunohistochemistry

Immunohistochemical staining was done as described previously [1, 30]. The anti-γ-H2AX antibody (Bethyl Laboratories, Montgomery, TX) was used to evaluate the double-strand breaks (DSB) level of DNA damage in the mouse HCC model. In each slide examined, we counted 1000 cells were from 6 fields with 200 × magnification. The percentage of positive cells, relative to total number of cells, was indicated on the y axis.

TUNEL assay

Apoptotic cells were detected with the In Situ Cell Death Detection kit (Roche, Indianapolis, IN), following the manufacturer's instructions, as described elsewhere [30]. Apoptotic cells (purple staining) were counted under a microscope. The apoptotic index was defined as the percentage of purple cells in the total number of cells in each sample. For each cell line analyzed, 200 cells were counted from the fields with 200 × magnification. As to each tumor sample analyzed, 1000 cells were counted from the fields with 200 × magnification. The experiments were repeated at least three times.

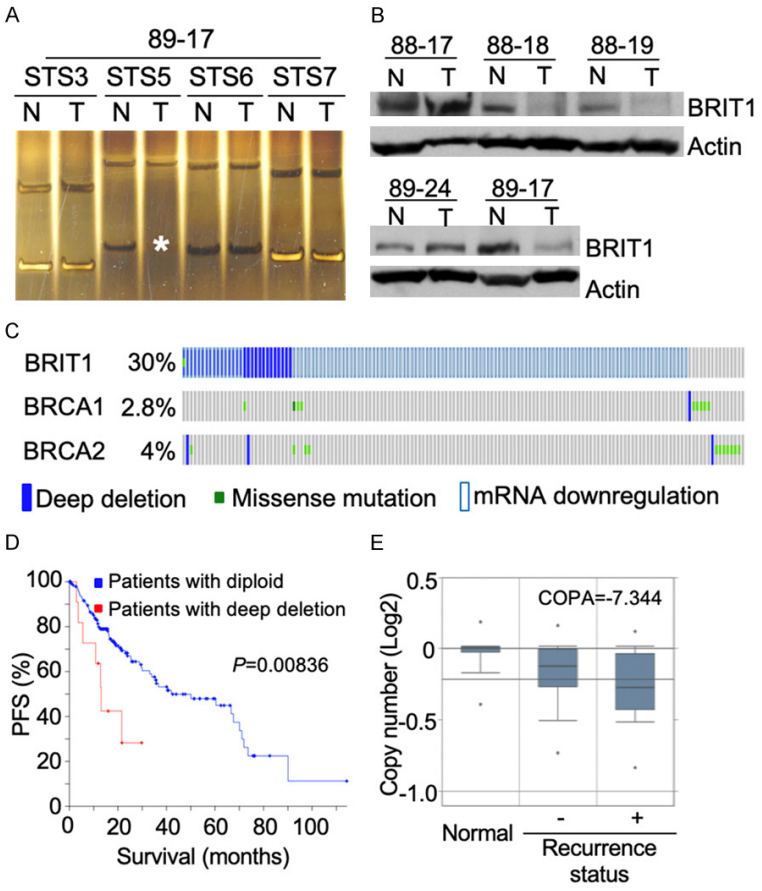

Figure 1. BRIT1 is aberrantly expressed and correlates with poor prognosis in HCC. A. Representative STS-based PCR analysis showed the presence of LOH in the BRIT1 locus in HCC sample 89-17 (n=3 technical repeats). STS3, STS5, STS6, and STS7 were 4 out of 13 sequence-tagged sites (STSs) used in this study. White star, lost band detected with STS5; N, non-cancerous liver tissue; T, HCC tumor tissue. LOH, loss of heterozygosity; STS, sequence-tagged site. B. Representative BRIT1 protein levels in 5 HCC samples (n=3 technical repeats). BRIT1 protein level was decreased in HCC samples as determined by Western blot analysis. C. BRIT1, but not BRCA1/2, was frequently altered in TCGA HCC samples (n=442). BRIT1 alterations include deep deletions, RNA downregulation, and mutations. For RNA expression level, z-score ≤-1.8. Data were retrieved from the cBioPortal as of June 27, 2017. D. BRIT1 deep deletion correlated with poor progression-free survival (PFS) of T1-stages TCGA HCC samples (n=186). HCC patients with diploid BRIT1, n=152 (with 62 relapsed), median =42.02; HCC patients with deep deletion of BRIT1, n=12 (with 7 relapsed), median =13.07. P=0.00836 with Log-rank test. E. BRIT1 low DNA copy number positively correlated with recurrence in the Guichard HCC cohort [34]. Normal, n=111; HCC samples without recurrence, n=27; HCC samples with recurrence, n=47. COPA=-7.344 with mCOPA analysis.

Statistical analysis

Statistical analysis was generally carried out using a two-tailed Student's t-Test. Kaplan-Meier survival curve and log-rank test were used for survival analysis. Error bars show s.d. P<0.05 was considered statistically significant. Cancer outlier profile analysis (COPA), a method developed for Oncomine [31], were used to identify the correlation of BRIT1 copy number with HCC recurrence in a subset of samples. At a given percentile cutoff (25% in this study), COPA scores representing the degree of BRIT1 under-expression in increasing subsets of cases.

Results

BRIT1 is aberrantly expressed in HCC and correlates with poor prognosis

To investigate whether BRIT1 is altered in HCC, we analyzed the loss of heterozigosity (LOH) of BRIT1 in a retrospective cohort of HCC patients (n=35) [10, 24]. As shown in Table S1, 40% (14 out of 35) of HCC samples exhibited LOH, represented by loss of at least one sequence tagged sites (STS) marker in the BRIT1 locus (**Figure 1A**). Meanwhile, BRIT1 protein level was reduced in 26% (9 out of 35) of HCC samples we tested (**Figure 1B**). To further assess BRIT1 aberrations in HCC, we retrieved the TCGA dataset via the cBioPortal for Cancer Genomics [26]. BRIT1's alterations occurred in about 30% of TCGA samples (n=442), including 7% with homozygous deletions, 27% with RNA downregulation with or without deletions, and 0.2% (1 in 442) with mutations, which were notably higher than the alteration rate of BRCA1/2 (**Figure 1C**), the two key HR repair genes frequently altered in breast or ovarian cancers [32]. This implicates BRIT1, instead of BRCA1/2, as the possible key HR protein commonly deleted and aberrantly expressed in HCC.

Furthermore, we investigated whether BRIT1 alterations are associated with poor prognosis

in HCC in the TCGA HCC samples (n=442) according to TCGA survival analysis standard [33]. BRIT1 homozygous deletion was found marginally correlated with poor prognosis of HCC samples (Figure S1). When we stratified the samples with tumor stage, BRIT1 deep deletion was associated with poor progression-free survival of HCC patients at T1 stage (n=186). For the T1 stage HCC patients, the median progression/relapse-free survival months for patients with diploid BRIT1 (62 out of 151 relapsed, median: 42.02) were significantly longer than those with BRIT1 deep deletion (7 out of 12 relapsed, median: 13.07) (**Figure 1D**), indicating that BRIT1 depletion was indeed positively correlated with poor prognosis of T1 stage HCC samples. Additionally, in the Guichard cohort [34], HCC samples with recurrence had a lower copy number of the BRIT1 gene than those without recurrence (**Figure 1E**), suggesting that low copy number of BRIT1 is linked to high incidence of HCC recurrence. Collectively these findings demonstrate that BRIT1 is frequently altered in HCC and its low copy number is positively correlated with poor prognosis.

BRIT1 mutation causes its dysfunction in HCC

To determine whether BRIT1 mutations occur in HCC, we initially screened the 35 pairs of HCC samples and adjacent tissues with PCR-based sequencing. We identified 1 mutation, K659fsX10 (**Figures 2A** and S2), which was located at the splicing acceptor site of intron 10, where A was mutated to G. This mutation disabled the common acceptor site AG, resulting in a deletion of AAAGCAG and a premature stop codon due to the usage of the nearest downstream cryptic acceptor site, thereby, producing a truncated protein lacking the tandem C-BRCTs of BRIT1 (**Figure 2A**). We ectopically expressed FLAG-tagged K659fsX10 in Hep3B cells and examined the capacity of IR-induced foci formation of this mutant to determine the dysfunction. As shown in **Figure 2B**, the wild-type BRIT1 formed DNA repair foci on damaged DNA, and these nuclear foci colocalized with γ-H2AX foci, an indicator for DSBs. However, K659fsX10 mutant could not relocate onto damaged DNA and failed to form DNA repair foci. Thus, the BRIT1 mutation abolishing its C-BRCT domain impaired BRIT1's DNA repair function and this type of mutation might influence the development of HCC.

BRIT1-deficient HCC cells are HR defective and hypersensitive to PARP inhibitors

In addition to clinical specimens, we assessed the BRIT1 status in HCC cell lines. As shown in **Figure 3A**, multiple cell lines including Hep3B and HepG2 had reduced DNA copy number of BRIT1 and reduced mRNA/protein level of BRIT1, while SNU449 cells maintained intact BRIT1 genome and protein expression. Thus, BRIT1 was proficient in SNU449 cells and deficient in Hep3B and HepG2 cells. We further adopted CRISPR/Cas9-mediated genome editing to generate BRIT1 knockout HCC cells using SNU449 (449.KO) and identified two cell clones, 449.KO1 and 449.KO2, in which the homozygous deletion of the BRIT1 locus was determined by genomic DNA-based PCR and sequencing, and the ablation of BRIT1 protein was confirmed by Western blot (**Figure 3B**). We and others have previously demonstrated that BRIT1 deficiency results in defective HR [4, 8]. Here, we validated that BRIT1-deficient HCC cells (Hep3B, HepG2, and 449.KO) rendered HR defects as compared to SNU449 by using DR-GFP/I-SceI-based HR repair assay (**Figure 3C**). These data indicate that BRIT1 is deficient in HCC cell lines and BRIT1 is indeed essential for maintaining high HR activity in HCC.

We then investigated whether HCC cells with BRIT1 deficiency-induced defective HR are vulnerable to PARPi that have been used for targeting BRCA1/2-associated HR deficiency [17, 21], We examined the inhibitory effect of PARPi on BRIT1-proficient and BRIT1-deficient HCC cells. Our study employed PARPi olaparib, which has entered clinical trials [21] and was recently approved by FDA for ovarian and breast cancer [35]. BRIT1-deficient Hep3B and HepG2 cells were more sensitive to olaparib than BRIT1-proficient SNU449 cells (**Figure 3D**). This inhibitory effect was also observed by using the PARPi AG014699 (Figure S3), suggesting that BRIT1 deficiency might contribute to hypersensitivity to PARPi. To validate the causal effect induced by BRIT1 deficiency, we employed three pairs of BRIT1-proficient and BRIT1-deficient cells to evaluate the cell-killing effect of olaparib. As shown in Figure S4, $BRIT1^{-/-}$ MEFs exhibited more sensitivity to olaparib

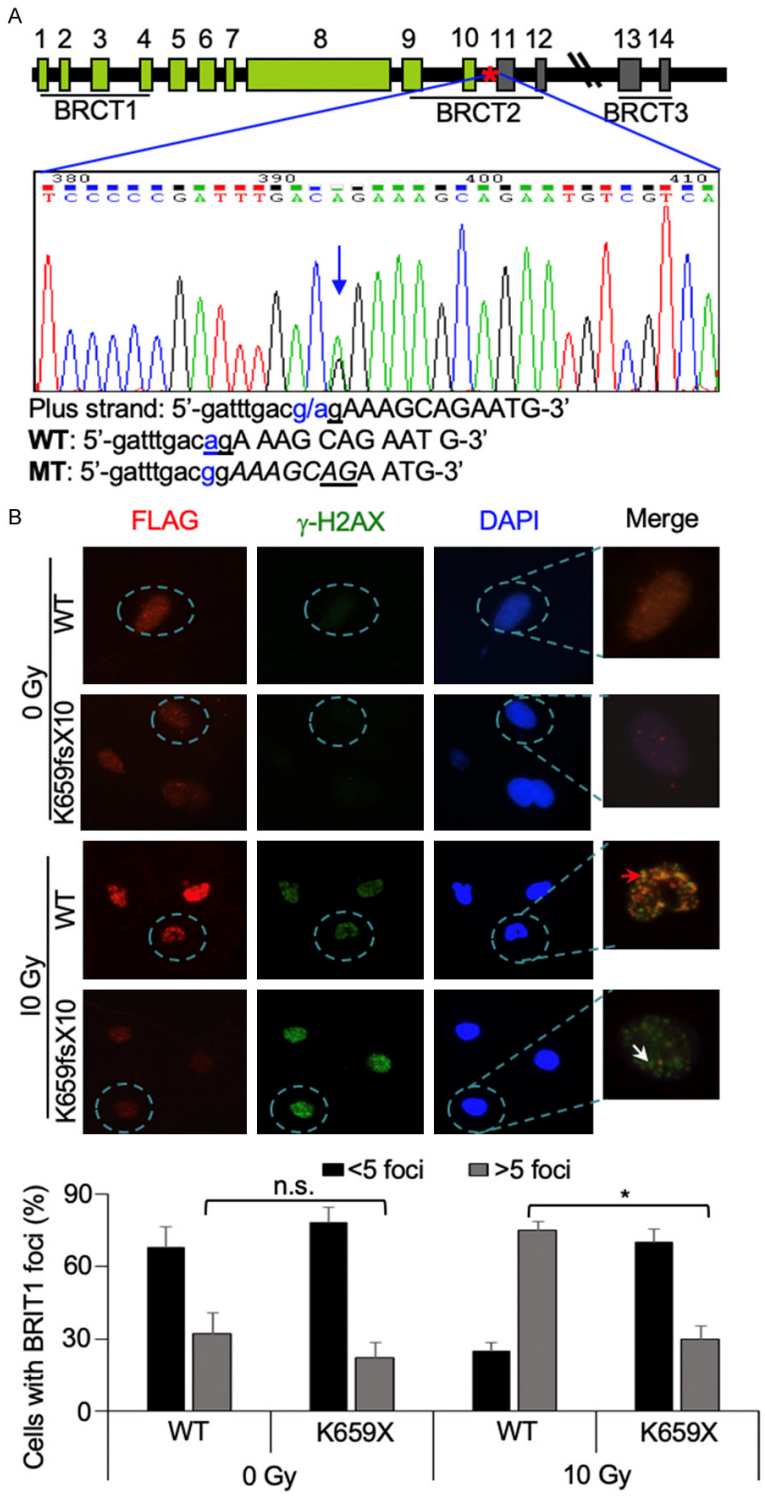

Figure 2. A splicing-acceptor mutant of BRIT1 is identified in HCC. A. BRIT1 mutant K659fsX10 identified in HCC sample 89-17 by PCR-based sequencing (n=3 technical repeats). Red star, position of K659fsX10; blue arrow, overlapping nucleotides including the normal and the mutant. WT, wild-type; MT, mutant. ag refers to the common acceptor site, and AG refers to the cryptic acceptor site. Italic *AAAGCAG* indicates the lost 7 nucleotides. B. Representative immunofluorescent staining showed that BRIT1 mutant K659fsX10 failed to localize onto the damaged DNA induced by IR. Bar graph illustrates the average percentage of cells with BRIT1 foci formation. At least 100 cells were counted for each condition from individual experiment (n=4 biological repeats). FLAG, FLAG-BRIT1. Red arrow, co-localization of BRIT1 and γ-H2AX; white arrow, no co-localization; n.s., not significant. *, P<0.05.

than BRIT1$^{+/+}$ MEFs. We further observed that BRIT1 knockout HCC cells (449.KO) were much more sensitive to olaparib than parental cells (**Figure 3E**). Additionally, we tested the cell response to PARPi after ectopic BRIT1 was restored in BRIT1-deficient Hep3B and HepG2 cells (i.e., Hep3B.BRIT1 vs Hep3B, and HepG2.BRIT1 vs HepG2). As expected, HepG2.BRIT1 and Hep3B.BRIT1 cells exhibited resistance to olaparib to some extent relative to the respective parental cells (**Figure 3F**). Altogether, these data indicated that BRIT1 deficiency indeed triggers hypersensitivity to PARPi in BRIT1-deficient HCC cells.

PI3Ki synergizes with PARPi to inhibit the survival of BRIT1-deficient HCC cells

Although PARPi is considered promising agents for targeting HR deficiency in BRCA1/2-carriers, resistance to these agents and relatively low efficacy have been reported [36]. We examined the effect of PARPi and other anti-cancer small compounds as a potential combination therapy targeting BRIT1-deficient HCC cells. It has been shown that the activity of the PI3K pathway is aberrantly high in HCC and this aberrant PI3K activation is crucial for the proliferation and survival of liver cells [37]. Thus, we selected

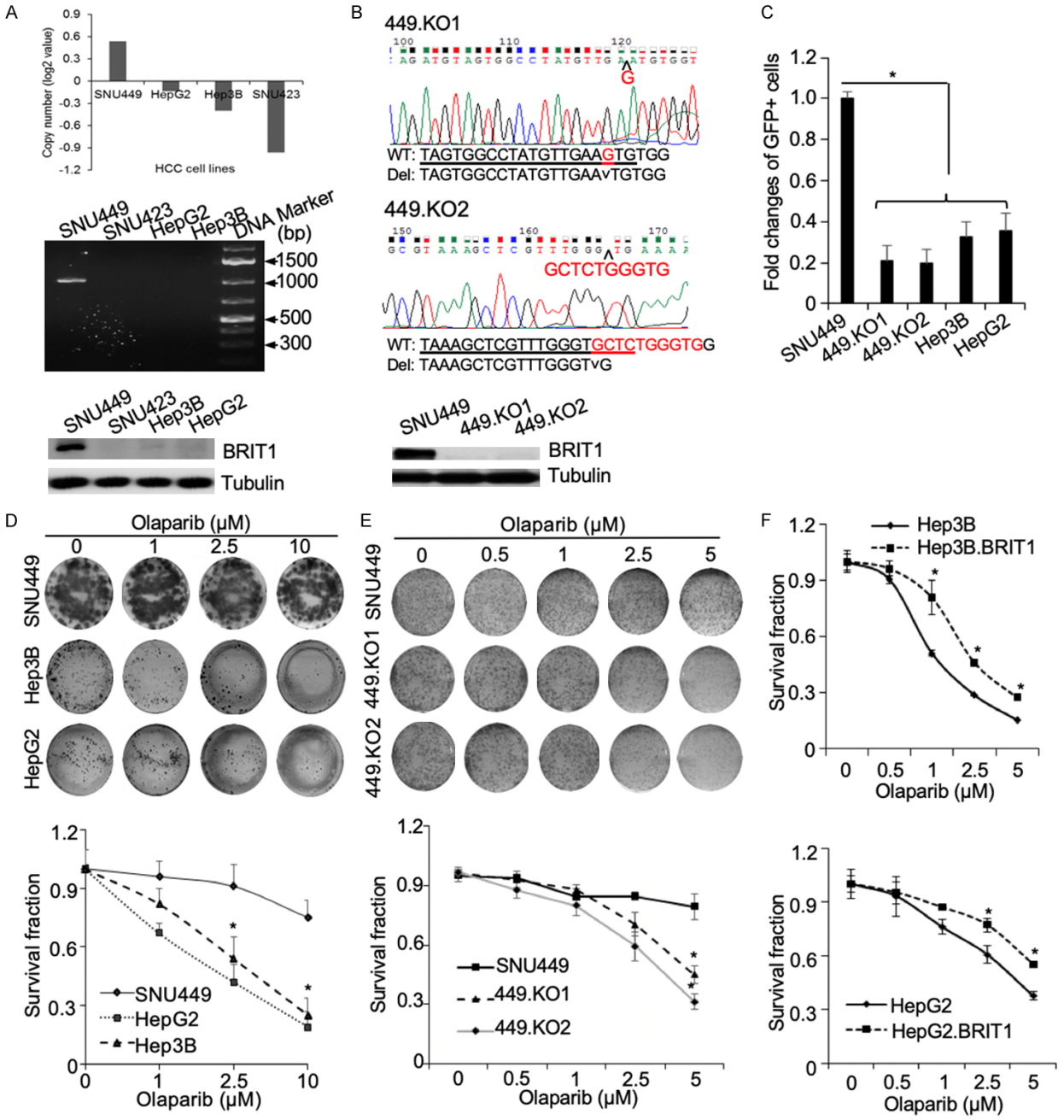
A
Copy number (log2 value)
SNU449
HepG2
Hep3B
SNU423
HCC cell lines
DNA Marker (bp)
1500
1000
500
300
BRIT1
Tubulin
B
449.KO1
WT: TAGTGGCCTATGTTGAAGTGTGG
Del: TAGTGGCCTATGTTGAAvTGTGG
449.KO2
GCTCTGGGTG
WT: TAAAGCTCGTTTGGGTGCTCTGGGTGG
Del: TAAAGCTCGTTTGGGTvG
C
Fold changes of GFP+ cells
449.KO1
449.KO2
D
Olaparib (μM)
E
F
Hep3B
Hep3B.BRIT1
Survival fraction
HepG2
HepG2.BRIT1

Figure 3. BRIT1-deficient cells are hypersensitive to PARP inhibitor. A. BRIT1 was proficient in SNU449 cells, but deficient in Hep3B and HepG2. DNA copy number retrieved from the Cancer Cell Line Encyclopedia (CCLE). The mRNA and protein levels determined by RT-PCR with the primers mentioned in the Methods section and Western blot analysis, respectively (n=3 biological repeats). B. Generation of BRIT1-knockout HCC cells (449.KO) by CRISPR/Cas9. The BRIT1 null mutations induced by two sets of guide RNA were validated by PCR-based sequencing, showing a 1-bp deletion on both alleles in 449.KO1, and a 10-bp deletion on both alleles in 449.KO2, and by Western blot analysis of BRIT1 protein. C. HR activity was reduced in BRIT1-deficient HCC cells. The HR activity was determined by using DR-GFP/I-SceI-based HR repair assay and represented by the relative percentage of GFP+cells in each cell type. It was calculated by subtracting the percentage of GFP+cells in I-SceI-transfected cells with that in control plasmid pCAGGS-transfected cells, followed by normalizing with transfection efficiency determined by pEGFP-C1 plasmid. Each value in the bar graph was relative to the percentage of GFP+cells in SNU449, which was set at 1, and the data were obtained from repeated experiments (n=3 biological repeats). *, P<0.05 compared to SNU449 cells. D. Colony formation assay (n=3 biological repeats) showed BRIT1-deficient Hep3B and HepG2 cells were sensitive to olaparib. *, P<0.05 compared to SNU449. E. Colony formation assay (n=3 biological repeats) showed BRIT1 knockout 449.KO cells exhibited the hypersensitivity to olaparib. *, P<0.05 compared to SNU449. F. Colony formation assay (n=3 biological repeats) showed ectopic BRIT1 induced the resistance of Hep3B and HepG2 cells to PARPi olaparib. Survival rate was also determined by colony formation assay. *, P<0.05 when compared to respective parental cells.

BEZ235, a potent inhibitor of PI3K and mTOR (PI3Ki), as a co-targeting agent for BRIT1-deficient HCC. As shown in Figure S5, BEZ235 alone inhibited greater cell growth of BRIT1-deficient HCC cells, including Hep3B, and HepG2 cells, as compared with BRIT1-proficient SNU449 cells. Olaparib in combination with BEZ235 remarkably enhanced the cell-killing effect in BRIT1-deficient Hep3B and HepG2 cells (**Figure 4A**). The synergistic effects of this combination treatment were determined using a combination index (CI) (Table S2). The CRISPR/Cas9-mediated BRIT1-null 449.KO1 and 449.KO2 cells also exhibited the synergistic effects induced by the combination of olaparib and BEZ235. In contrast, SNU449 control cells (**Figure 4B**) were not sensitive to the experimental combination therapy. Further, we examined whether ectopic expression of BRIT1 can alleviate the inhibitory effect of these inhibitory agents in BRIT1-deficient HCC cells. As shown in **Figure 4C**, ectopic BRIT1 in Hep3B. BRIT1 and HepG2.BRIT1 cells partially reversed the synergistic effects induced by olaparib plus BEZ235 in Hep3B and HepG2 cells. Accordingly, the apoptotic rates of BRIT1-deficient cells Hep3B, HepG2, and 449.KO1 and 449.KO2 treated with olaparib plus BEZ235 were remarkably higher than those in SNU449 cells (**Figure 4D**). Collectively, these findings indicate that BRIT1 deficiency in HCC might be effectively targeted by PARPi in combination with PI3Ki.

PI3Ki and PARPi cooperate to induce DNA damage in BRIT1-deficient HCC cells

Loss of BRIT1 results in genomic instability due to defective HR and NHEJ repair machinery [4, 8], and BRIT1-deficient cells harbor high rates of DNA damage and are sensitized to the inhibition of alternative DNA repair involving PARP, as described in **Figure 3**. Accordingly, we found that olaparib induced more DSBs in BRIT1-deficient cells (449.KO2 and Hep3B) than BRIT1-proficient cells (SNU449 and Hep3B. BRIT1) as determined with neutral-pH comet assay (**Figure 5A** and **5B**, OLA panels). γ-H2AX foci (another marker for DSBs) were elevated in BRIT1-deficient cells, as compared with BRIT1-proficient cells (**Figure 5C** and **5D**, OLA panels), and this effect correlated with diminishing PARP activity (the reduced level of PAR) (**Figure 5E**). Notably, olaparib significantly elevated activity of the PI3K pathway (phosphorylation of AKT) (**Figure 5E**), suggesting that upregulation of PI3K pathway may compensate for DNA repair in the context of BRIT1 and PARP deficiency.

To elucidate the mechanisms underlying the synergy effects of PI3Ki combined with PARPi, we next investigated the possibility that the high sensitivity of BRIT1-deficient HCC cells to PI3Ki is the consequence of an undescribed role for the PI3K pathway in facilitating DNA repair. Indeed, we found that BEZ235 alone induced more DSBs (as determined by neutral-pH comet assay and γ-H2AX foci staining) in BRIT1-deficient cells than BRIT1-proficient cells (**Figure 5A-D**, BEZ panels), and that this correlated with drastically decreased AKT phosphorylation (**Figure 5F**), suggesting the PI3K pathway is indeed involved in DNA repair mechanisms under BRIT1 deficiency. BEZ235 caused a dose-dependent increase in the level of PAR paralleling the decrease in AKT phosphorylation (**Figure 5F**). Thus, we could infer that reciprocal interaction between PI3K pathway and

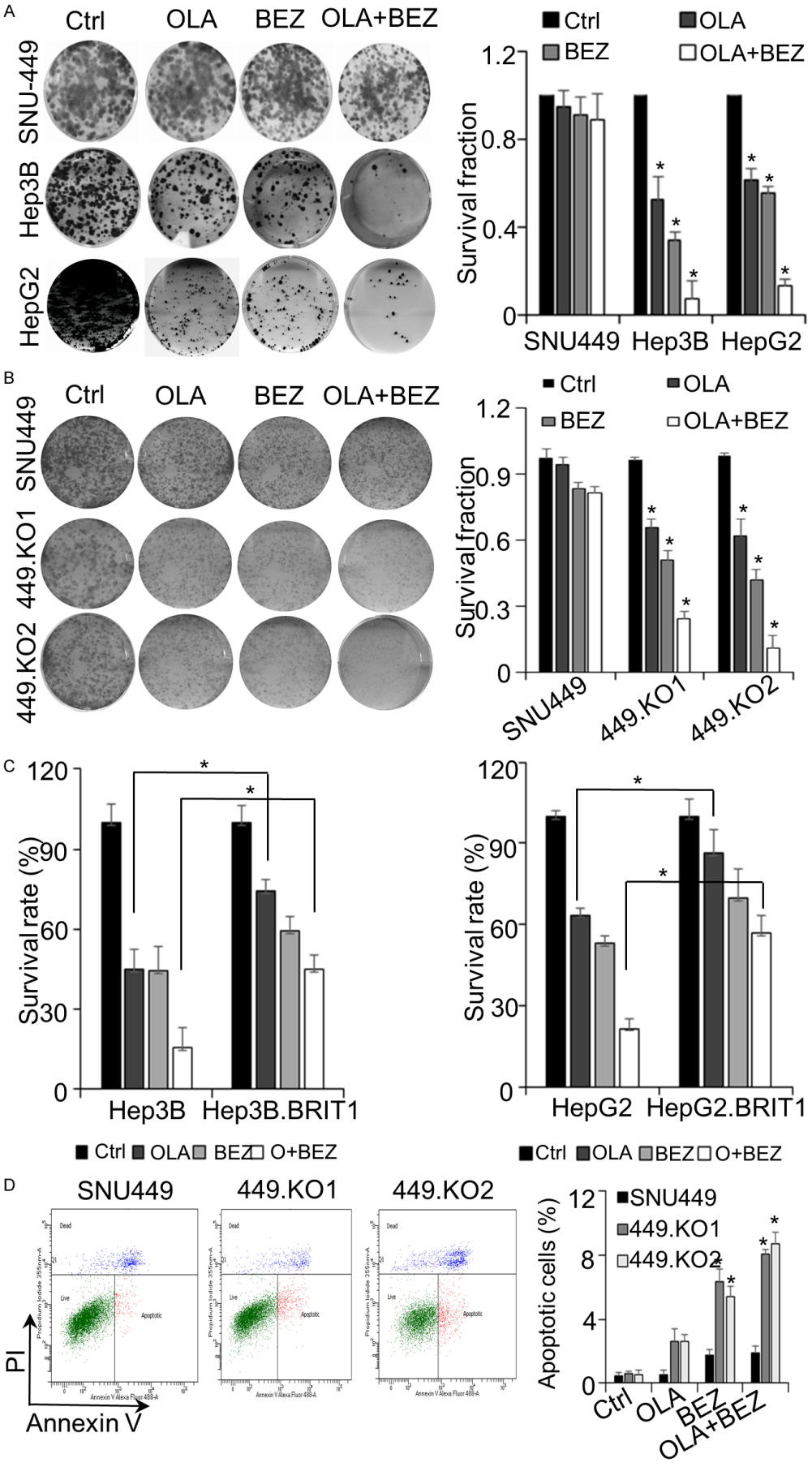
A
Ctrl
OLA
BEZ
OLA+BEZ
SNU-449
Hep3B
HepG2
Survival fraction
SNU449
Hep3B
HepG2
B
SNU449
449.KO1
449.KO2
C
Survival rate (%)
Hep3B
Hep3B.BRIT1
HepG2
HepG2.BRIT1
D
PI
Annexin V
Apoptotic cells (%)

Figure 4. PARP inhibitor synergizes with PI3K inhibitor to suppress BRIT1-deficient HCC in vitro. A. Colony formation assay showed BRIT1-deficient HCC cells Hep3B and HepG2 exhibited the synergy of PARPi and PI3Ki. Cells were treated with PARPi olaparib (2.5 μM) and PI3Ki BEZ235 (2.5 nM) alone or in combination for 2 weeks, and the inhibitory effects were determined by using colony formation assay (n=3 biological repeats). *, P<0.05 compared to control. B. Colony formation assay showed BRIT1 ablation by CRISPR/Cas9 enhanced the synergy of olaparib and BEZ235 in HCC cells (n=3 biological repeats). *, P<0.05 compared to control. C. Colony formation assay showed ectopic BRIT1 attenuated the synergistic effect of olaparib and BEZ235 (n=3 biological repeats). *, P<0.05. D. Apoptotic rate was increased in BRIT1-deficient cells treated with olaparib or BEZ235 alone, and further enhanced by the combination. Ctrl, control; OLA, olaparib; BEZ, BEZ235; OLA (or O)+BEZ, combination of olaparib and BEZ235. *, P<0.05 compared to SNU449 cells.

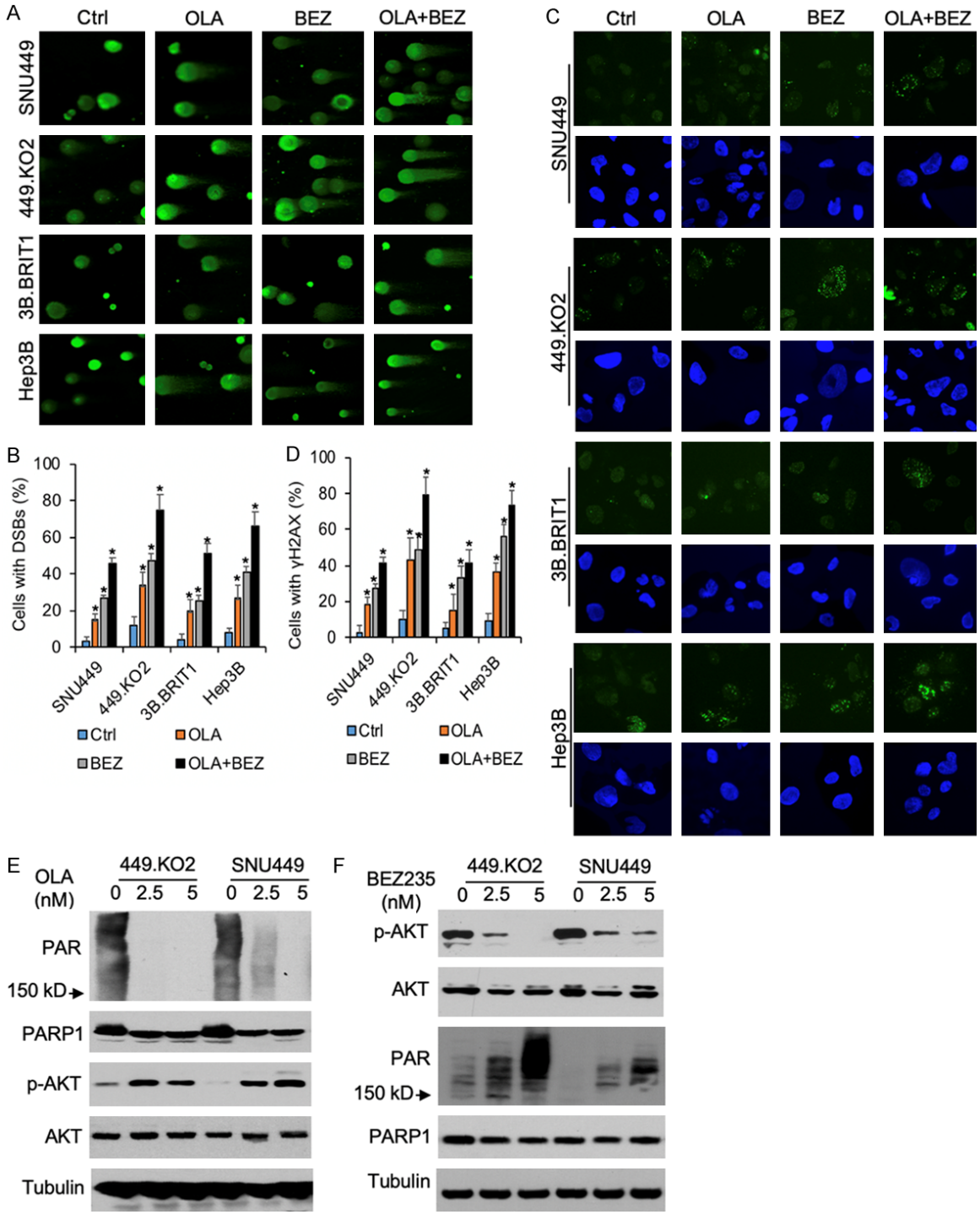

Figure 5. DNA damage is significantly induced by PARP inhibitor and PI3K inhibitor. A and B. DSBs were induced by olaparib and BEZ235 alone and exaggerated by combination treatment in BRIT1-deficient 449.KO2 and Hep3B cells. A. Representative neutral-pH comet assay of DNA damage. B. Quantitative analysis of ~100 cells for each condition (n=3 biological repeats). More than 97% untreated SNU449 cells contained tail moments <2, which was set as the parameter for cells with intact DNA. Cells with the parameter >2 were regarded as the one with DSBs. Ctrl, control; OLA, olaparib. BEZ, BEZ235; OLA+BEZ, olaparib+BEZ235. *, P<0.05. C and D. γ-H2AX foci were significantly elevated by treatment of olaparib or BEZ235 alone and aggravated by combination treatment in BRIT1-deficient 449.KO2 and Hep3B cells. C. Representative γ-H2AX immunofluorescent staining of γ-H2AX foci. D. Quantitative analysis of ~100 cells for each condition (n=3 biological repeats). *, P<0.05. E. Western blot analysis showed that olaparib induced a high level of phosphor-AKT in BRIT1-deficient cells (n=5 biological repeats). OLA, olaparib; PAR, poly (ADP-ribose); p-AKT, phosphorylated AKT. *, P<0.05. F. Western blot analysis demonstrated that BEZ235 induced a high level of PAR formation in BRIT1-deficient cells (n=5 biological repeats). PAR, poly (ADP-ribose); p-AKT, phosphorylated AKT. *, P<0.05.

PARP may compensate for the inhibitory effects to facilitate DNA repair. As a consequence, dual treatment with olaparib and BEZ235 markedly increased the level of DSBs than single treatment, and exacerbated the degree of DNA damage in BRIT1-deficient HCC cells when compared to BRIT1-proficient cells (**Figure 5A-D**, OLA+BEZ panels). Collectively, these observations suggest that interaction between PI3K pathway and the PARP-related pathway facilitate compensatory DNA repair in the context of BRIT1 deficiency.

BRIT1-deficient tumor growth is inhibited by PARPi alone or in combination with PI3Ki in vivo

To assess the inhibitory effect of PARPi on BRIT1-deficient HCC in vivo, we used BRIT1-deficient Hep3B cells and their BRIT1-reexpressing counterparts Hep3B.BRIT1 cells to establish xenograft tumors in nude mice. Nude mice with xenografts reaching up to ~100 mm^3 were randomly separated into 2 groups treated with or without olaparib (olaparib and control) once each day for 2 weeks. Hep3B tumor growth was significantly decreased in the olaparib group as compared to controls (**Figure 6A**). Likewise, after the olaparib-treated mice were sacrificed at the end of treatment, Hep3B tumor weight was also found to be notably decreased (**Figure 6B**). Accordingly, PARP enzyme activity (reflected by the PAR level) was accordingly decreased in olaparib-treated tumors (**Figure 6C**). In contrast, Hep3B.BRIT1 xenografts exhibited the resistance to olaparib (Figure S6). Thus, these data showed that BRIT1-deficient tumors are selectively sensitive to PARPi, and this subset of HCC can be inhibited by PARPi alone in vivo.

To assess whether PI3Ki exaggerates the inhibitory effect of PARPi on xenograft tumor growth in vivo, the mice with HCC tumors were treated with BEZ235, olaparib, or the combination of these two drugs. As shown in **Figure 6D**, tumors derived from BRIT1-deficient Hep3B cells were sensitive to olaparib or BEZ235 alone, and importantly tumor growth was substantially inhibited when a combination of olaparib and BEZ235 was administered, supporting our findings in vitro with cultured cells (**Figure 4**). BRIT1-proficient HCC tumors derived from Hep3B.BRIT1 exhibited resistance to olaparib, and there was no significant inhibitory effect resulting from the combinational treatment (Figure S6). Furthermore, relative to the control, olaparib, and BEZ235 groups, the tumors that received the combinational treatment showed a dramatic increase in γ-H2AX foci formation, and the apoptotic rate in the combined treatment group was higher than that in the single treatment or control, as determined by TUNEL assay (**Figure 6E**). Altogether, our studies showed that PI3Ki can augment the inhibitory effect and DNA damage effect of PARPi, and a combination therapy of PARPi and PI3Ki can potently suppress tumors with BRIT1 deficiency in vivo.

Discussion

To our knowledge, this is the first report that identifies BRIT1 as a key DNA repair protein altered in HCC. Incidence of HCC has risen over last 20 years. Several risk factors for HCC are known, including hepatitis B and hepatitis C virus (HBV/HCV) infection, diabetes mellitus, obesity, and alcohol abuse [38]. A recent comprehensive analysis of HCC identifies several genomic alterations that influence the development of HCC at the genetic level, including mutations in the TERT gene promoter (44%), and mutations in the CTNNB1 (β-catenin) (26%) and TP53 (31%) genes [39]. However, mutations in other genes, like DNA repair genes, are relatively rare in this type of cancer. Intriguingly, our study shows that, although its mutation

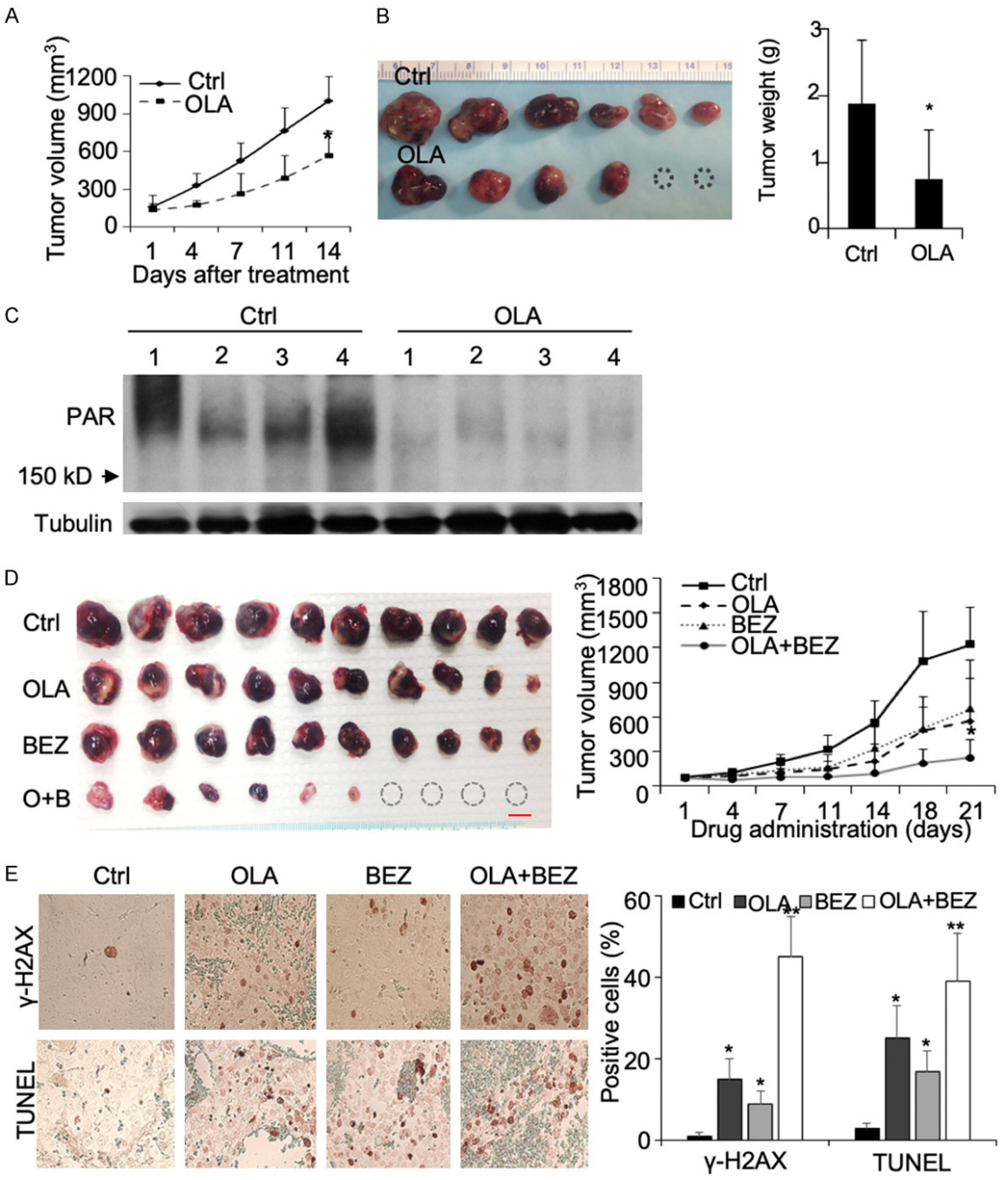

Figure 6. BRIT1-deficient xenograft tumor growth is remarkably inhibited by PARP inhibitor in combination with PI3K inhibitor in vivo. A. BRIT1-deficient Hep3B tumor growth was deterred by olaparib (n=6 for each group) as compared to control. *, P<0.05. B. Macroscopical images showed that Hep3B xenograft tumor growth was attenuated by olaparib (n=6 mice each group). Bar graph, the average tumor weight after sacrifice. *, P<0.05 when compared to control. C. Western blot analysis demonstrated that PAR formation was abolished by olaparib in Hep3B xenograft tumors (n=3 biological repeats). D. Macroscopical images (left) and bar graph of tumor volume (right) demonstrated that tumor growth of Hep3B xenografts was remarkably inhibited by olaparib and BEZ235 in combination (n=10 mice each group). *, P<0.05 compared to control. E. Representative γ-H2AX staining and apoptotic cells in Hep3B xenografts tumors showed that combination treatment of olaparib and BEZ235 remarkably triggered γ-H2AX foci intensity and apoptosis. γ-H2AX foci formation was determined by immunohistochemistry, and apoptotic cells were stained by using TUNEL assay (n=3 mice for each condition). *, P<0.05 compared with control or single drug treatment.

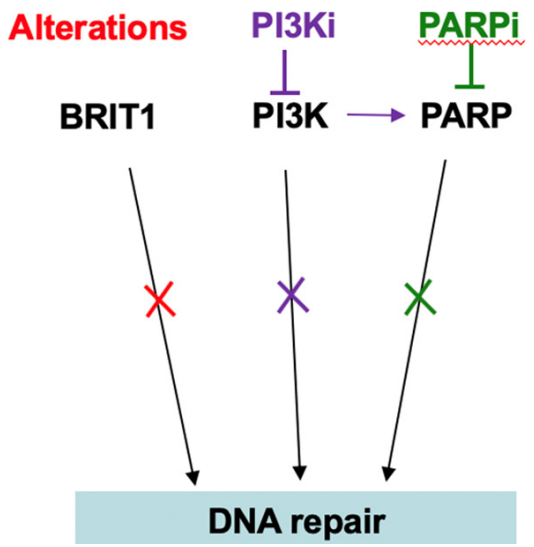

Figure 7. Schematic diagram of the proposed model illustrates the enhanced synthetic lethality achieved by co-targeting of PARPi and PI3Ki in BRIT1-deficient HCC. In BRIT1-deficient HCC, BRIT1 deficiency causes DNA damage. Under this condition, PARP inhibition by PARPi leads to the increase of DNA damage, accompanied with a high PI3K/AKT activity for compensatory DNA repair. Meanwhile, PI3K inhibition by PI3Ki leads to the accumulation of DNA damage as well as an increased PARP activity. As such, concurrent inhibition of PI3K and PARP remarkably enhances the synthetic lethality under BRIT1 deficiency, leading to much more severe DNA damages than in the context of BRIT1 proficiency.

rate is low, BRIT1 LOH, including deep deletion (homozygous deletion) and its RNA/protein deficiency, is frequently observed in the HCC samples studied. Our analysis reveals that BRIT1 alteration rate is 30% including 7% deep deletion and this deletion is positively correlated with poor prognosis of HCC patients. The influence of BRIT1 deficiency on HCC development is further supported by our two mouse models. We generated the knockout mice with BRIT1 deleted specifically in liver, and this hepatic ablation of BRIT1 significantly accelerates the PTEN-null induced HCC development (unpublished data). Furthermore, global ablation of BRIT1 promotes lymphoma formation in p53 null mice where BRIT1 deficiency caused substantial chromosomal aberrations via abolishing HR and NHEJ repair [8, 9]. Thus, these genetic studies in mice and clinical samples indicate that BRIT1 can function as a novel tumor suppressor for HCC via preserving its genomic stability.

Currently, the mechanisms underlying BRIT1 low or absent expression in HCC are not fully understood. The high frequency of LOH or homozygous deletion identified in this study (**Figure 1**) suggest that these aberrations may significantly promote the low or absent BRIT1 levels in tumors. In oral squamous carcinoma, BRIT1 promoter hypermethylation is observed in 10% of the cases and its 3'-UTR also harbors two functional seed regions for miR-27a which negatively regulate its level [40], suggesting that promoter hypermethylation and microRNA regulation are alternative mechanisms for BRIT1 downregulation. Thus, although BRIT1's mutation rate is low, homozygous deletion, LOH, promoter hypermethylation, microRNA transcriptional regulation and/or probably protein stability may all contribute to BRIT1 deficiency in HCC.

It is worth mentioning that, although allelic loss is a major type of BRIT1 aberrations in HCC, we identified one mutation K659fsX10 that destroyed the C-BRCT domains and abolished its localization onto the damaged DNA sites (**Figure 2**). This result was in agreement with previous data showing that C-BRCTs are crucial to the capacity of BRIT1 to form IR-induced nuclear foci and execute DNA repair [41, 42]. Mutations of BRIT1 have been previously reported, including p.Ser25X, p.Thr27Arg, p.Val50Gly, p.Ser72Leu, and p.Trp75Arg [43-45], which were identified in type 1 primary microcephaly [43] and/or premature chromosome condensation (PCC) syndrome [46]. Most of these mutations resided in and usually destroyed/modulated the N-BRCT domain, which is mainly responsible for mitotic entry, PCC, and DNA recombination repair under some circumstances [5, 43, 44, 47]. These N-BRCT mutations did not appear to be associated with cancer predisposition due to hypomorphic mutations or redundant complemented pathways [48]. Based on a TCGA-related study published recently BRIT1 mutations in HCC samples are rare [49]. Nevertheless, BRIT1 mutations/variations affecting the C-BRCTs have been observed in a wide range of cancers, although their individual potential functions have not been fully characterized (Figure S7). While occurring infrequently in HCC, BRIT1 mutations with disruptive C-BRCTs might be implicated in promoting HCC.

Our present data (**Figures 4** and **6**) add BRIT1 to the list of HR genes whose deficiencies confer high sensitivity to PARP inhibitors. The various cell models used in this study, including ablation of BRIT1 in BRIT1-proficient cells (SNU449 and MEF) and restoration of BRIT1 in BRIT1-deficient cells (Hep3B and HepG2), demonstrate that BRIT1 is critical for maintaining high HR capacity and that its deficiency potentiates PARPi cytotoxicity in HCC. Our findings are in agreement with our and others' prior studies showing that BRIT1 can interact and recruit RAD51 and BRCA2 onto DSBs for HR repair [4, 8], and interact with chromatin remodeling protein complex (SWI/SNF) and increase the access of the repair proteins to the DNA damage sites via relaxation of chromatin structure [5, 47]. These activities might demonstrate the mechanisms underlying BRIT1's integral role in HR repair.

Among the HR proteins associated with cancer, BRCA1/2, whose mutations mainly occur in breast and ovarian cancers [50], have been well-studied. PARPi was originally developed to target BRCA1/2-associated HR defects in these two cancers. Studies show that tumor cells lacking other components of the HR pathway (e.g., RAD51) are also sensitive to PARPi due to HR defects [51]. However, in HCC, these HR proteins including BRCA1/2 and RAD51 are rarely aberrantly expressed or mutated. On the other hand, our analysis from our own samples and the TCGA dataset reveal that BRIT1 is the DNA repair protein exhibiting the most aberration rate in HCC among all the DNA proteins analyzed. Moreover, the level of PARP in HCC is significantly higher than that in normal liver tissues, and PARP inhibition decreases the growth of liver tumors [52]. We identified a 30% aberration rate of BRIT1 and demonstrates BRIT1 deficiency role in HR incompetency and PARPi sensitization. These critical findings could greatly facilitate expanding the rational usage of PARPi-based targeting therapy to treat HR-deficient HCC.

Of note, we observed a remarkable synergistic effect from the combination of PARPi (olaparib) with PI3Ki (BEZ235) that inhibited BRIT1-deficient HCC in vitro and in vivo and uncovered a mechanism for this synergy on tumor suppression. In the context of BRIT1 deficiency, PARP inhibition by PARPi leads to increased DNA damage accompanied by high PI3K/AKT activities as compensatory DNA repair (**Figure 5**). Inactivation of PI3K by BEZ235 triggers both DSB and SSB accompanied with elevated PARP activity and their DNA damage is further enhanced with the addition of PARPi in BRIT1-deficient HCC (**Figure 5**). Our observations are consistent with prior studies showing that PI3K activity can influence DNA repair; PI3Kα inactivation by BKM120 enhances the recruitment of RAD51 onto DSBs and sensitizes cells to PARPi [53], and PI3Kβ is required for recruitment of NSB1 to the damage sites and assembly of repair foci in response to IR [54]. Given that BRIT1 is essential for competent HR repair [4, 8], an intact or elevated PI3K signaling becomes more critical for proper DNA repair in BRIT1-deficient cells, and therefore, a plausible mechanism of synergy could be proposed as follows: PARP inhibition in BRIT1-deficient HCC induces the accumulation of DSBs, which might be partially repaired by the induction of high PI3K activity; when co-targeted with BEZ235, which further inhibits DNA repairs by inactivation of PI3K, BRIT1-deficient cells can accumulate substantially more DNA damages, resulting in enhanced synthetic lethality of PARPi and BRIT1 deficiency (**Figure 7**). We surmise that the substantially enhanced DNA damage induced by co-targeting with olaparib and BEZ235 can at least partially explain the synergistic action of this dual treatment.

Accordingly, using PARPi in combination with PI3Ki as an adjuvant therapy for HCC may provide significant clinical benefits. Emerging evidence shows that single agent therapies have limited efficacies partially due to tumors cells' adaptive mechanisms leading to drug resistance soon after exposure. In the case of PARPi therapy, patients with BRCA1/2-associated cancer respond well to olaparib or other PARPi [17, 21]. However, tumor treated with PARPi can acquire treatment resistance resulting from the hyper-activation of PI3K signaling, elevation of mTOR activity, or restoration of HR capacity by loss of p53BP1 [55]. In the case of PI3Ki treatment, BEZ235 clinical trial as a single agent does not result in favorable patient outcome, which is attributable to drug resistance developed by increasing PARP activity and triggering the feedback loop of this pathway [56]. Also, at the single agent dose, BEZ235 exhibits toxicity in patients. It is conceivable that the lower dose combination therapy as demonstrated here might reduce treatment-induced toxicity and

also overcome the drug resistance from the single agent (either PARPi or PI3Ki). In the process of our study, more potent PARPi (e.g., BMN673) have being successfully developed to target HR-deficient cancer [57]. Also, new versions of PI3Ki with high specificity are being explored in clinical trials. We expect combination therapy using more potent and less toxic PARPi and PI3Ki to hold great promise in treating HCC with HR deficiency in the future.

In summary, our findings establish for the first time that BRIT1 is a key HR repair protein altered in HCC. BRIT1 deletion correlates with worse outcome of HCC patients. BRIT1-deficient HCC are HR-defective and selectively hypersensitive to PARPi. Combination therapy with PARPi and PI3Ki results in synergistic suppression of BRIT1-deficient HCC, both in vitro and in vivo mouse model. Mechanistically, PARPi or PI3Ki can induce substantial DNA damages and make cells more dependent on PI3K or PARP activity, respectively. Our study dissects BRIT1 dysfunction in HCC and lays a scientific foundation for rationally expanding the usage of PARPi in the treatment of HCC with BRIT1 deficiency, which may eventually guide personalized use of PARPi and PI3Ki in the clinic for treating unresectable HCC.

Acknowledgements

Financial support statement: This project was supported by the grants from the National Institutes of Health (to KL, NIH R21-CA161513 and NIH R01-CA155151-01), a Pilot Project Grant from the Dan L. Duncan Cancer Center at Baylor College of Medicine (to KL), the St. Luke's Hospital McDonald Research Foundation Award (to KL), and a Faculty Research Seed Award from the Department of Surgery at Baylor College of Medicine (to YL). The authors would like to thank Dr. Thomas D. Schmittgen (Ohio State University, Columbus, OH) for his kindly providing us HCC cell lines (SNU-449, SNU-423, and SNU-182). We also thank Drs. Ana María Rodríguez and Kimberly Macellaro, members of the Michael E. DeBakey Department of Surgery Research Core Team at Baylor College of Medicine, for their assistance in editing during the preparation of this manuscript.

Disclosure of conflict of interest

None.

Address correspondence to: Dr. Shiaw-Yih Lin, Department of System Biology, MD Anderson Cancer Center, 6565 MD Anderson Blvd., Houston, TX 77030, USA. Tel: 713-563-4217; E-mail: sylin@mdanderson.org; Dr. Kaiyi Li, Department of Tharocic Head and Neck Medical Oncology, MD Anderson Cancer Center, Houston, TX, USA. E-mail: kli5@mdanderson.org

References

[1] Rai R, Dai H, Multani AS, Li K, Chin K, Gray J, Lahad JP, Liang J, Mills GB, Meric-Bernstam F and Lin SY. BRIT1 regulates early DNA damage response, chromosomal integrity, and cancer. Cancer Cell 2006; 10: 145-157.

[2] Wood JL, Singh N, Mer G and Chen J. MCPH1 functions in an H2AX-dependent but MDC1-independent pathway in response to DNA damage. J Biol Chem 2007; 282: 35416-35423.

[3] Jeffers LJ, Coull BJ, Stack SJ and Morrison CG. Distinct BRCT domains in Mcph1/Brit1 mediate ionizing radiation-induced focus formation and centrosomal localization. Oncogene 2008; 27: 139-144.

[4] Wu X, Mondal G, Wang X, Wu J, Yang L, Pankratz VS, Rowley M and Couch FJ. Microcephalin regulates BRCA2 and Rad51-associated DNA double-strand break repair. Cancer Res 2009; 69: 5531-5536.

[5] Peng G, Yim EK, Dai H, Jackson AP, Burgt I, Pan MR, Hu R, Li K and Lin SY. BRIT1/MCPH1 links chromatin remodelling to DNA damage response. Nat Cell Biol 2009; 11: 865-872.

[6] Gruber R, Zhou Z, Sukchev M, Joerss T, Frappart PO and Wang ZQ. MCPH1 regulates the neuroprogenitor division mode by coupling the centrosomal cycle with mitotic entry through the Chk1-Cdc25 pathway. Nat Cell Biol 2011; 13: 1325-1334.

[7] Manke IA, Lowery DM, Nguyen A and Yaffe MB. BRCT repeats as phosphopeptide-binding modules involved in protein targeting. Science 2003; 302: 636-639.

[8] Liang Y, Gao H, Lin SY, Peng G, Huang X, Zhang P, Goss JA, Brunicardi FC, Multani AS, Chang S and Li K. BRIT1/MCPH1 is essential for mitotic and meiotic recombination DNA repair and maintaining genomic stability in mice. PLoS Genet 2010; 6: e1000826.

[9] Liang Y, Gao H, Lin SY, Goss JA, Du C and Li K. Mcph1/Brit1 deficiency promotes genomic instability and tumor formation in a mouse model. Oncogene 2015; 34: 4368-4378.

[10] Becker SA, Zhou YZ and Slagle BL. Frequent loss of chromosome 8p in hepatitis B virus-positive hepatocellular carcinomas from China. Cancer Res 1996; 56: 5092-5097.

[11] Lu T, Hano H, Meng C, Nagatsuma K, Chiba S and Ikegami M. Frequent loss of heterozygosity in two distinct regions, 8p23.1 and 8p22, in hepatocellular carcinoma. World J Gastroenterol 2007; 13: 1090-1097.
[12] Bray F, Ferlay J, Soerjomataram I, Siegel RL, Torre LA and Jemal A. Global cancer statistics 2018: GLOBOCAN estimates of incidence and mortality worldwide for 36 cancers in 185 countries. CA Cancer J Clin 2018; 68: 394-424.
[13] Siegel RL, Miller KD and Jemal A. Cancer statistics, 2019. CA Cancer J Clin 2019; 69: 7-34.
[14] Farazi PA and DePinho RA. Hepatocellular carcinoma pathogenesis: from genes to environment. Nat Rev Cancer 2006; 6: 674-687.
[15] Siegel RL, Miller KD and Jemal A. Cancer statistics, 2015. CA Cancer J Clin 2015; 65: 5-29.
[16] Attwa MH and El-Etreby SA. Guide for diagnosis and treatment of hepatocellular carcinoma. World J Hepatol 2015; 7: 1632-1651.
[17] Bryant HE, Schultz N, Thomas HD, Parker KM, Flower D, Lopez E, Kyle S, Meuth M, Curtin NJ and Helleday T. Specific killing of BRCA2-deficient tumours with inhibitors of poly(ADP-ribose) polymerase. Nature 2005; 434: 913-917.
[18] Schreiber V, Dantzer F, Ame JC and de Murcia G. Poly(ADP-ribose): novel functions for an old molecule. Nat Rev Mol Cell Biol 2006; 7: 517-528.
[19] De Soto JA and Deng CX. PARP-1 inhibitors: are they the long-sought genetically specific drugs for BRCA1/2-associated breast cancers? Int J Med Sci 2006; 3: 117-123.
[20] Murai J, Huang SY, Das BB, Renaud A, Zhang Y, Doroshow JH, Ji J, Takeda S and Pommier Y. Trapping of PARP1 and PARP2 by clinical PARP inhibitors. Cancer Res 2012; 72: 5588-5599.
[21] Fong PC, Boss DS, Yap TA, Tutt A, Wu P, Mergui-Roelvink M, Mortimer P, Swaisland H, Lau A, O'Connor MJ, Ashworth A, Carmichael J, Kaye SB, Schellens JH and de Bono JS. Inhibition of poly(ADP-ribose) polymerase in tumors from BRCA mutation carriers. N Engl J Med 2009; 361: 123-134.
[22] Slagle BL, Zhou YZ and Butel JS. Hepatitis B virus integration event in human chromosome 17p near the p53 gene identifies the region of the chromosome commonly deleted in virus-positive hepatocellular carcinomas. Cancer Res 1991; 51: 49-54.
[23] Slagle BL, Zhou YZ, Birchmeier W and Scorsone KA. Deletion of the E-cadherin gene in hepatitis B virus-positive Chinese hepatocellular carcinomas. Hepatology 1993; 18: 757-762.
[24] Nguyen NT, Cotton RT, Harring TR, Guiteau JJ, Gingras MC, Wheeler DA, O'Mahony CA, Gibbs RA, Brunicardi FC and Goss JA. A primer on a hepatocellular carcinoma bioresource bank using the cancer genome atlas guidelines: practical issues and pitfalls. World J Surg 2011; 35: 1732-1737.
[25] Sheu JC, Lin YW, Chou HC, Huang GT, Lee HS, Lin YH, Huang SY, Chen CH, Wang JT, Lee PH, Lin JT, Lu FJ and Chen DS. Loss of heterozygosity and microsatellite instability in hepatocellular carcinoma in Taiwan. Br J Cancer 1999; 80: 468-476.
[26] Cerami E, Gao J, Dogrusoz U, Gross BE, Sumer SO, Aksoy BA, Jacobsen A, Byrne CJ, Heuer ML, Larsson E, Antipin Y, Reva B, Goldberg AP, Sander C and Schultz N. The cBio cancer genomics portal: an open platform for exploring multidimensional cancer genomics data. Cancer Discov 2012; 2: 401-404.
[27] Chou TC and Talalay P. Quantitative analysis of dose-effect relationships: the combined effects of multiple drugs or enzyme inhibitors. Adv Enzyme Regul 1984; 22: 27-55.
[28] Takahashi N, Li W, Banerjee D, Guan Y, Wada-Takahashi Y, Brennan MF, Chou TC, Scotto KW and Bertino JR. Sequence-dependent synergistic cytotoxicity of ecteinascidin-743 and paclitaxel in human breast cancer cell lines in vitro and in vivo. Cancer Res 2002; 62: 6909-6915.
[29] Stoppoloni D, Canino C, Cardillo I, Verdina A, Baldi A, Sacchi A and Galati R. Synergistic effect of gefitinib and rofecoxib in mesothelioma cells. Mol Cancer 2010; 9: 27.
[30] Liang Y, Gao H, Lin SY, Goss JA, Brunicardi FC and Li K. siRNA-based targeting of cyclin E overexpression inhibits breast cancer cell growth and suppresses tumor development in breast cancer mouse model. PLoS One 2010; 5: e12860.
[31] Tomlins SA, Rhodes DR, Perner S, Dhanasekaran SM, Mehra R, Sun XW, Varambally S, Cao X, Tchinda J, Kuefer R, Lee C, Montie JE, Shah RB, Pienta KJ, Rubin MA and Chinnaiyan AM. Recurrent fusion of TMPRSS2 and ETS transcription factor genes in prostate cancer. Science 2005; 310: 644-648.
[32] Nielsen FC, van Overeem Hansen T and Sørensen CS. Hereditary breast and ovarian cancer: new genes in confined pathways. Nat Rev Cancer 2016; 16: 599-612.
[33] Liu J, Lichtenberg T, Hoadley KA, Poisson LM, Lazar AJ, Cherniack AD, Kovatich AJ, Benz CC,Levine DA, Lee AV, Omberg L, Wolf DM, Shriver CD, Thorsson V and Hu H; Cancer Genome Atlas Research Network. An integrated TCGA pan-cancer clinical data resource to drive high-quality survival outcome analytics. Cell 2018; 173: 400-416, e411.
[34] Guichard C, Amaddeo G, Imbeaud S, Ladeiro Y, Pelletier L, Maad IB, Calderaro J, Bioulac-Sage P, Letexier M, Degos F, Clement B, Balabaud C,

Chevet E, Laurent A, Couchy G, Letouze E, Calvo F and Zucman-Rossi J. Integrated analysis of somatic mutations and focal copy-number changes identifies key genes and pathways in hepatocellular carcinoma. Nat Genet 2012; 44: 694-698.

[35] Slade D. PARP and PARG inhibitors in cancer treatment. Genes Dev 2020; 34: 360-394.

[36] Henneman L, van Miltenburg MH, Michalak EM, Braumuller TM, Jaspers JE, Drenth AP, de Korte-Grimmerink R, Gogola E, Szuhai K, Schlicker A, Bin Ali R, Pritchard C, Huijbers IJ, Berns A, Rottenberg S and Jonkers J. Selective resistance to the PARP inhibitor olaparib in a mouse model for BRCA1-deficient metaplastic breast cancer. Proc Natl Acad Sci U S A 2015; 112: 8409-8414.

[37] Nakanishi K, Sakamoto M, Yamasaki S, Todo S and Hirohashi S. Akt phosphorylation is a risk factor for early disease recurrence and poor prognosis in hepatocellular carcinoma. Cancer 2005; 103: 307-312.

[38] Gomaa AI, Khan SA, Toledano MB, Waked I and Taylor-Robinson SD. Hepatocellular carcinoma: epidemiology, risk factors and pathogenesis. World J Gastroenterol 2008; 14: 4300-4308.

[39] Llovet JM, Montal R, Sia D and Finn RS. Molecular therapies and precision medicine for hepatocellular carcinoma. Nat Rev Clin Oncol 2018; 15: 599-616.

[40] Venkatesh T, Nagashri MN, Swamy SS, Mohiyuddin SM, Gopinath KS and Kumar A. Primary microcephaly gene MCPH1 shows signatures of tumor suppressors and is regulated by miR-27a in oral squamous cell carcinoma. PLoS One 2013; 8: e54643.

[41] Xu X, Lee J and Stern DF. Microcephalin is a DNA damage response protein involved in regulation of CHK1 and BRCA1. J Biol Chem 2004; 279: 34091-34094.

[42] Lin SY, Rai R, Li K, Xu ZX and Elledge SJ. BRIT1/MCPH1 is a DNA damage responsive protein that regulates the Brca1-Chk1 pathway, implicating checkpoint dysfunction in microcephaly. Proc Natl Acad Sci U S A 2005; 102: 15105-15109.

[43] Jackson AP, Eastwood H, Bell SM, Adu J, Toomes C, Carr IM, Roberts E, Hampshire DJ, Crow YJ, Mighell AJ, Karbani G, Jafri H, Rashid Y, Mueller RF, Markham AF and Woods CG. Identification of microcephalin, a protein implicated in determining the size of the human brain. Am J Hum Genet 2002; 71: 136-142.

[44] Trimborn M, Richter R, Sternberg N, Gavvovidis I, Schindler D, Jackson AP, Prott EC, Sperling K, Gillessen-Kaesbach G and Neitzel H. The first missense alteration in the MCPH1 gene causes autosomal recessive microcephaly with an extremely mild cellular and clinical phenotype. Hum Mutat 2005; 26: 496.

[45] Ghani-Kakhki M, Robinson PN, Morlot S, Mitter D, Trimborn M, Albrecht B, Varon R, Sperling K and Neitzel H. Two missense mutations in the primary autosomal recessive microcephaly gene MCPH1 disrupt the function of the highly conserved N-Terminal BRCT domain of microcephalin. Mol Syndromol 2012; 3: 6-13.

[46] Trimborn M, Bell SM, Felix C, Rashid Y, Jafri H, Griffiths PD, Neumann LM, Krebs A, Reis A, Sperling K, Neitzel H and Jackson AP. Mutations in microcephalin cause aberrant regulation of chromosome condensation. Am J Hum Genet 2004; 75: 261-266.

[47] Wood JL, Liang Y, Li K and Chen J. Microcephalin/MCPH1 associates with the Condensin II complex to function in homologous recombination repair. J Biol Chem 2008; 283: 29586-29592.

[48] Leung JW, Leitch A, Wood JL, Shaw-Smith C, Metcalfe K, Bicknell LS, Jackson AP and Chen J. SET nuclear oncogene associates with microcephalin/MCPH1 and regulates chromosome condensation. J Biol Chem 2011; 286: 21393-21400.

[49] Cancer Genome Atlas Research Network. Electronic address wbe and Cancer Genome Atlas Research Network. Comprehensive and integrative genomic characterization of hepatocellular carcinoma. Cell 2017; 169: 1327-1341, e1323.

[50] King MC, Marks JH and Mandell JB; New York Breast Cancer Study Group. Breast and ovarian cancer risks due to inherited mutations in BRCA1 and BRCA2. Science 2003; 302: 643-646.

[51] McCabe N, Turner NC, Lord CJ, Kluzek K, Bialkowska A, Swift S, Giavara S, O'Connor MJ, Tutt AN, Zdzienicka MZ, Smith GC and Ashworth A. Deficiency in the repair of DNA damage by homologous recombination and sensitivity to poly (ADP-ribose) polymerase inhibition. Cancer Res 2006; 66: 8109-8115.

[52] Shiobara M, Miyazaki M, Ito H, Togawa A, Nakajima N, Nomura F, Morinaga N and Noda M. Enhanced polyadenosine diphosphate-ribosylation in cirrhotic liver and carcinoma tissues in patients with hepatocellular carcinoma. J Gastroenterol Hepatol 2001; 16: 338-344.

[53] Juvekar A, Burga LN, Hu H, Lunsford EP, Ibrahim YH, Balmana J, Rajendran A, Papa A, Spencer K, Lyssiotis CA, Nardella C, Pandolfi PP, Baselga J, Scully R, Asara JM, Cantley LC and Wulf GM. Combining a PI3K inhibitor with a PARP inhibitor provides an effective therapy for BRCA1-related breast cancer. Cancer Discov 2012; 2: 1048-1063.

[54] Kumar A, Fernandez-Capetillo O and Carrera AC. Nuclear phosphoinositide 3-kinase beta

controls double-strand break DNA repair. Proc Natl Acad Sci U S A 2010; 107: 7491-7496.
[55] Kim Y, Kim A, Sharip A, Jiang J, Yang Q and Xie Y. Reverse the resistance to PARP inhibitors. Int J Biol Sci 2017; 13: 198-208.
[56] Pons-Tostivint E, Thibault B and Guillermet-Guibert J. Targeting PI3K signaling in combination cancer therapy. Trends Cancer 2017; 3: 454-469.
[57] Litton JK, Rugo HS, Ettl J, Hurvitz SA, Gonçalves A, Lee KH, Fehrenbacher L, Yerushalmi R, Mina LA, Martin M, Roché H, Im YH, Quek RGW, Markova D, Tudor IC, Hannah AL, Eiermann W and Blum JL. Talazoparib in patients with advanced breast cancer and a germline BRCA mutation. N Engl J Med 2018; 379: 753-763.
[58] Wang C, Taciroglu A, Maetschke SR, Nelson CC, Ragan MA and Davis MJ. mCOPA: analysis of heterogeneous features in cancer expression data. J Clin Bioinforma 2012; 2: 22.

Table S1. Loss of heterozygosity (LOH) at the BRIT1 locus in a small group of HCC samples[a]

Samples		Sequence-tagged sites (STS)												
		S1[b]	S2	S3	S4	S5	S6	S7	S8	S9	S10	S11	S12	S13
88-04	N[c]	-[d]	nd[e]	-	nd	-	-	nd	-	-	-	nd	-	-
	T	-	nd	-	nd	-	-	nd	-	+	-	nd	-	-
88-12	N	-	nd	-	-	-	-	-	-	-	-	-	-	-
	T	-	nd	-	-	-	-	-	-	-	-	-	-	-
89-05	N	-	nd	-	nd	-	-	-	-	-	-	-	nd	-
	T	-	nd	-	nd	-	-	-	-	-	-	-	nd	-
89-07	N	-	-	-	nd	-	-	nd	-	-	-	-	-	-
	T	-	-	+	nd	-	+	nd	-	+	-	+	-	-
89-16	N	-	nd	-	-	-	-	-	-	-	nd	nd	nd	nd
	T	-	nd	-	-	-	-	-	-	-	nd	nd	nd	nd
89-17	N	-	-	-	nd	-	-	-	-	-	nd	nd	nd	nd
	T	-	-	-	nd	-	-	+	-	-	nd	nd	nd	nd
89-21	N	-	nd	-	nd	-	-	-	-	-	nd	nd	nd	nd
	T	-	nd	-	+	-	-	-	-	-	nd	nd	nd	nd
89-24	N	-	nd	-	nd	-	-	-	-	-	nd	nd	nd	nd
	T	-	nd	-	nd	+	-	-	-	-	nd	nd	nd	nd
89-25	N	-	nd	-	nd	-	-	-	-	-	-	-	-	-
	T	-	nd	-	nd	-	-	-	-	-	-	-	-	-
89-33	N	-	nd	-	-	-	-	-	-	-	-	-	-	-
	T	-	nd	-	-	-	-	-	-	+	-	+	-	-
06-14	N	-	nd	-	nd	nd	-	-	-	-	-	-	-	-
	T	-	nd	-	nd	nd	-	-	-	-	-	-	-	-
06-25	N	-	-	-	-	nd	-	-	-	-	-	-	-	-
	T	-	-	-	-	nd	-	-	-	-	-	-	-	-
06-26	N	-	nd	-	-	nd	-	-	-	-	-	-	-	-
	T	-	nd	-	-	nd	-	-	-	-	-	-	-	-
07-32	N	-	nd	-	nd	-	-	-	nd	-	-	-	-	-
	T	-	nd	+	nd	+	-	-	nd	-	-	-	-	+
07-33	N	-	nd	-	nd	-	-	-	nd	-	-	-	-	-
	T	-	nd	-	nd	-	-	-	nd	-	-	-	-	-
07-34	N	-	nd	-	nd	-	-	-	-	-	-	-	-	-
	T	+	nd	+	nd	+	+	+	+	+	+	+	+	+
07-35	N	-	nd	-	nd	-	-	-	-	-	-	-	-	-
	T	-	nd	-	nd	-	-	-	-	-	-	-	-	-

Note: *a,* The samples which are not informative for loss of heterozygosity (LOH) are not included in the table. *b,* All the sequence-tagged site (STS, S) names are provided in the Supplementary Experimental Procedures section. *c,* N, nontumorous tissue; T, tumor tissue. *d,* Minus (-) indicates that the pattern of the bands is the one in nontumorous tissue or the same as that in non-tumorous tissue; Plus (+) means the loss of certain bands in tumor tissue compared with non-tumorous tissue, i.e. LOH positive. *e,* nd, not determined.

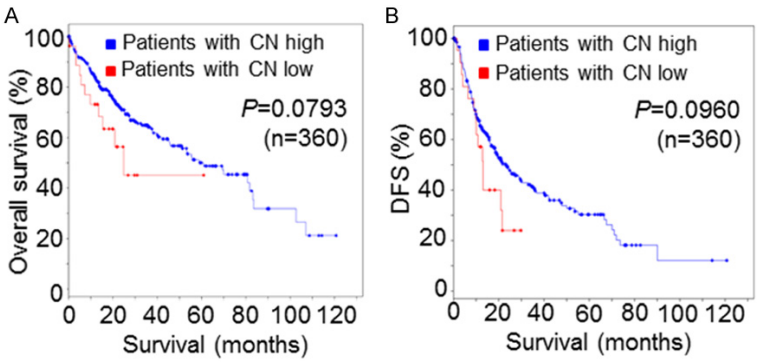

Figure S1. BRIT1 low copy number is marginally correlated with poor overall survival (A) and disease-free survival (B) in TCGA HCC samples. These data were retrieved from TCGA by using cBioPortal for Cancer Genomics with default putative copy-number alterations from GISTIC (Genomic Identification of Significant Targets in Cancer) on September 18, 2017, and updated on March 12, 2020. CN, copy number; DFS, disease-free survival.

A

```
Query  1861  ATACAGTGGAAGTGTTAAAAATAGACCAACAAGGCATGATGTTTTAGATGACTCATGTGA  1920
             ||||||||||||||||||||||||||||||||||||||||||||||||||||||||||||
Sbjct  1891  ATACAGTGGAAGTGTTAAAAATAGACCAACAAGGCATGATGTTTTAGATGACTCATGTGA  1950

Query  1921  CGGCTTTAAGGACCTCATCAAACCTCATGAGGAATTGAAGAAAAGTGGGAGAGGCAAAAA  1980
             ||||||||||||||||||||||||||||||||||||||||||||||||||||||||||||
Sbjct  1951  CGGCTTTAAGGACCTCATCAAACCTCATGAGGAATTGAAGAAAAGTGGGAGAGGCAAAAA  2010

Query  1981  GCCAACAAGAACATTAGTCATGACAAGCATGCCATCTGA-------AATGTCGTCATCCA  2033
             ||||||||||||||||||||||||||||||||||||||       |||||||||||||||
Sbjct  2011  GCCAACAAGAACATTAGTCATGACAAGCATGCCATCTGAAAAAGCAGAATGTCGTCATCCA  2070

Query  2034  GGTTGTGGATAAATTGAAAGGCTTTTCAATTGCACCAGACGTCTGTGAGACCACGACTCA  2093
             ||||||||||||||||||||||||||||||||||||||||||||||||||||||||||||
Sbjct  2071  GGTTGTGGATAAATTGAAAGGCTTTTCAATTGCACCAGACGTCTGTGAGACCACGACTCA  2130

Query  2094  CGTGCTTTCCGGGAAGCCACTTCGCACCCTGAATGTGCTGCTGGGAATTGCGCGTGGCTG  2153
             ||||||||||||||||||||||||||||||||||||||||||||||||||||||||||||
Sbjct  2131  CGTGCTTTCCGGGAAGCCACTTCGCACCCTGAATGTGCTGCTGGGAATTGCGCGTGGCTG  2190
```

Query: K659fsX10 mutant
Subject: intact BRIT1 (Accession # NM_024596)

B

TGAGTGTAACTGCTTTGATGGGCATGTGCAACAAAG

TCATTCATTTTGTTAATTTTTCCCCCGATTTGACGGA

AAG CAG***A ATG TCG TCA TCC AGG TTG TGG ATA***

AAT TGA AAGGCTTTTCAATTGCACCAGACGTCT

GTGAGACCACGACTCACGTGCTTTCCGGGAAGCCA

CTTCGCACCCTGAATGTGCTGCTGGGAATT

Figure S2. Partial sequence of the identified BRTI1 mutant p.K659MdelfsX10. A. Partial cDNA sequence of BRIT1 mutant p.K659MdelfsX10 (or K659fsX10). This mutant was detected in HCC sample 89-17 with a 7-bp deletion

(red line). The whole K659fsX10 mutant cDNA sequence was deposited in GenBank (accession # KU674825). B. Partial genomic sequence spanning intron 10 and exon 11 of the BRIT1 gene in HCC sample 89-17. The sequence was deposited (GenBank accession # KU550240). Yellow-highlighted letters indicate the partial genomic sequence of intron 10, including the mutant GG (green-shaded letters) from the canonical splicing acceptor site AG (i.e. A>G). The underlined represent the partial remaining sequence of exon 11. Red letters, the 7 lost nucleotides; blue-shaded red letters AG, the encrypted splicing acceptor site in the 5' end of exon 11; letters in italics, the potential codons; red-shaded TGA, the premature stop codon used in K659fsX10.

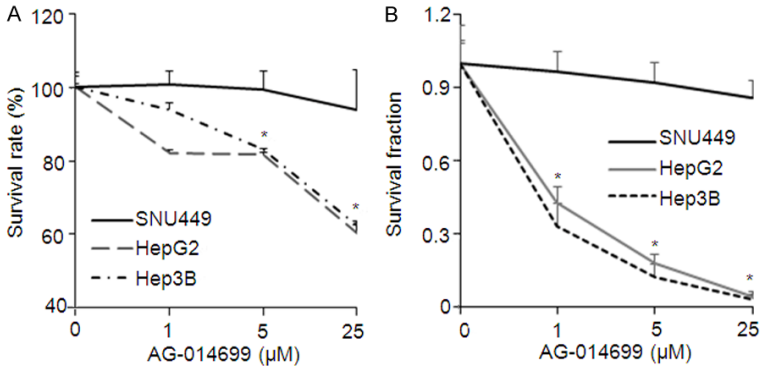

Figure S3. BRIT1-low cells are sensitive to PARP inhibitor AG-014699. (A and B) BRIT1-deficient cells Hep3B and HepG2 were more sensitive to AG-014699 than BRIT1-proficient cells SNU449. The survival rate was determined with the CCK-8 cell proliferation assay (A) and the colony formation assay (B). *, P<0.05, when compared with SNU449.

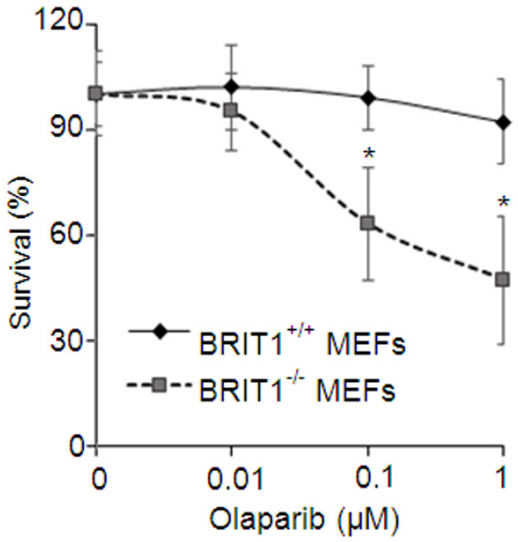

Figure S4. BRIT1$^{-/-}$ MEF cells are sensitive to PARP inhibitor olaparib. The cells were seeded into 96-well plates, and the survival rate was determined with the CCK-8 cell proliferation assay. *, P<0.05, when compared with BRIT1$^{+/+}$ MEF cells.

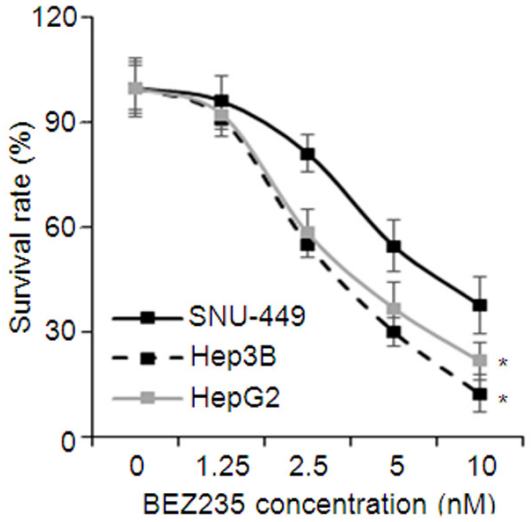

Figure S5. BRIT1-deficient cells Hep3B and HepG2 are sensitive to PI3K inhibitor BEZ235. The cells were seeded into 96-well plates, and the survival rate was determined with the CCK-8 cell proliferation assay. *, P<0.05, when compared with BRIT1-proficient cells SNU-449.

Table S2. Combination index (CI) chart for combinational therapy of olaparib and BEZ235

Cell lines	Schedule	Fraction of Inhibition	CI	Synergistic Effect?
Hep3B	2.5 μM OLA+1.25 nM BEZ	0.66	0.53	Yes
	1.25 μM OLA+2.5 nM BEZ	0.80	0.44	Yes
HepG2	2.5 μM OLA+1.25 nM BEZ	0.69	0.77	Yes
	1.25 μM OLA+2.5 nM BEZ	0.75	0.64	Yes
SNU-449	2.5 μM OLA+1.25 nM BEZ	0.25	>0.9	No
	1.25 μM OLA+2.5 nM BEZ	0.33	>0.9	No

Note: OLA, PARP inhibitor olaparib; BEZ, PI3K inhibitor BEZ235; CI, combination index.

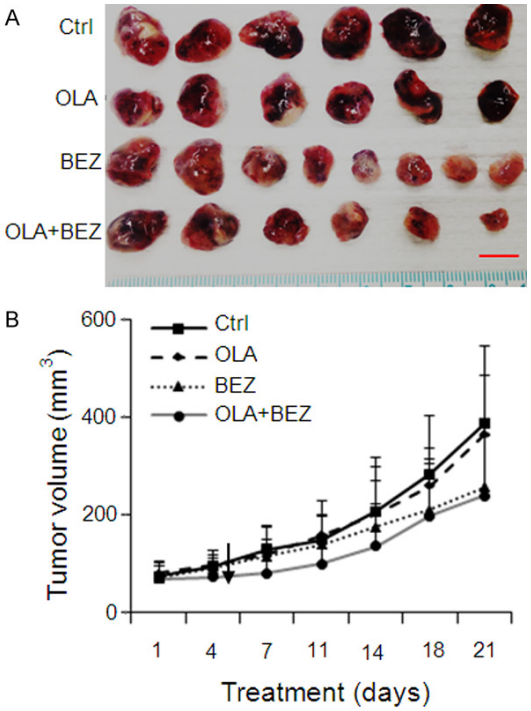

Figure S6. BRIT1-overexpressing Hep3B tumors show resistance to olaparib and are less susceptible to the synergistic effect of olaparib and BEZ235 in the *in vivo* xenograft tumor model. A. Representative images of BRIT1-overexpressing Hep3B (Hep3B.BRIT1) xenograft tumors treated for 3 weeks with olaparib, BEZ235, olaparib+BEZ235, or control vehicle. B. Volume of Hep3B.BRIT1 tumors during treatment with olaparib, BEZ235, olaparib+BEZ235, or control. Ctrl, control; OLA, olaparib; BEZ, BEZ235; OLA+BEZ, combination treatment of olaparib and BEZ235. Scale bar, 10 mm.

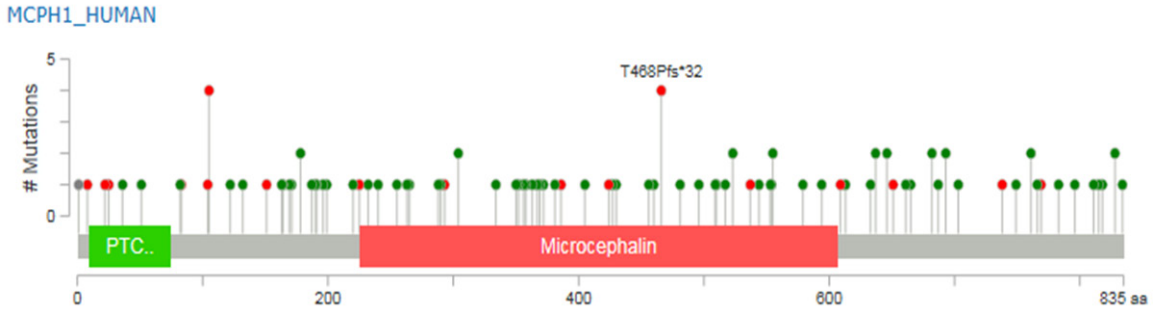

Figure S7. BRIT1 mutations occurred in multiple human cancers. BRIT1 mutations reported by TCGA in multiple human cancers were retrieved with cBioPortal for Cancer Genomics on September 12, 2018. MCPH1, also known as BRIT1. TCGA, The Cancer Genome Atlas.